PROCEEDINGS OF SCIENCE

Recent Developments in Heavy-Ion Theory: Soft and Hard Probes

Shanshan Cao[a,*]

[a] *Institute of Frontier and Interdisciplinary Science, Shandong University, Qingdao, Shandong 266237, China*

E-mail: shanshan.cao@sdu.edu.cn

A brief theory overview on quark-gluon plasma (QGP) produced in relativistic heavy-ion collisions is presented. Thermal statistical model and hydrodynamic model have been shown to be successful tools to study hadron spectra at low (soft) transverse momentum; while perturbative QCD calculation, corrected with non-perturbative interactions between partons and a thermal medium, has been found essential in understanding heavy quark and high transverse momentum jet (hard) spectra. Using these sophisticated model calculations, reasonable extractions of various properties of the QGP have been achieved, such as its initial geometry, transport coefficients and equation of state. Better constraints on additional information, such as in-medium hadron structure, evolution profile of electromagnetic field and pattern of jet-induced medium excitation in high-energy nuclear collisions, are expected with more precise measurements at LHC and RHIC in the near future.

The Eleventh Annual Conference on Large Hadron Collider Physics (LHCP2023)
22-26 May 2023
Belgrade, Serbia

*Speaker

© Copyright owned by the author(s) under the terms of the Creative Commons Attribution-NonCommercial-NoDerivatives 4.0 International License (CC BY-NC-ND 4.0).

PoS(LHCP2023)210

1. Introduction

The major goal of relativistic heavy-ion programs at the CERN Large Hadron Collider (LHC) and the BNL Relativistic Heavy-Ion Collider (RHIC) is to understand properties of QCD at extremely high density and temperature. Lattice QCD predicts a rapid increase of the energy density of the QCD matter as its temperature increases across a critical value, indicating the release of quark-gluon degrees of freedom from the hadron gas [1, 2]. This highly excited state of matter is called "quark-gluon plasma" (QGP) [3–6]. Major questions of heavy-ion physics include: What is the initial state of collisions and how does this initial state thermalize into the QGP? What are the thermal and transport properties of the QGP? How do energetic particles interact with the QGP? And how does color deconfined state transit into confined state? Challenges of heavy-ion theory include the non-perturbative nature of QCD and the many-body problem.

In general, probes of the QGP can be categorized into soft and hard ones. The former is low transverse momentum ($p_{\rm T}$) hadrons emitted from the QGP on its hadronization hypersurface [7, 8]; while the latter includes heavy quarks [9, 10] and high-$p_{\rm T}$ jets [11–14] that are mainly produced from the initial hard scatterings and then plough through the QGP. In this work, we will discuss some recent developments on constraining the QGP properties using these soft and hard probes.[1]

2. Soft probes

The simplest observable in heavy-ion collisions is the soft hadron yield. In Ref. [16], one sees a surprisingly good description of the yields of different hadron species using the thermal statistical model, indicating these hadrons are close to thermal equilibrium when being produced. By integrating the Boltzmann distribution over the phase space, we can get the number of particles (with species i) as a function of its spin degeneracy g_i, baryon chemical potential μ_i and mass m_i, and the effective volume V and temperature T of the medium as

$$N_i = \frac{g_i V T^3}{2\pi^2} e^{\mu_i/T} \frac{m_i^2}{T^2} K_2\left(\frac{m_i}{T}\right), \tag{1}$$

with K_2 representing the modified Bessel function of the second kind. This formula can then be fit to the experimental data on the particle yields, from which one may extract the hadronization temperature and baryon chemical potential at a given beam energy, and in the end obtain the phase boundary between the hadronic matter and the QGP in the (T-μ) phase diagram of QCD as the beam energy (or μ) varies. Despite its successful performance, the thermal model is limited by its lack of dynamic information about the QGP evolution and its inapplicability to non-thermalized observables at high $p_{\rm T}$.

The second observable is collective flow coefficients of soft hadrons. As illustrated in the left panel of Fig. 1, the overlapping region between the two colliding nuclei is anisotropic in the transverse plane (the plane perpendicular to the beam direction). On average, this region has an almond shape in non-central collisions, with its asymmetry quantified by the elliptic eccentricity

[1] Electromagnetic probes [15], including photons and dileptons that are produced in either the initial hard scatterings or thermal radiation during the whole evolution of the nuclear matter, are another valuable tool for exploring the QGP. This is beyond the scope of this work.

PoS(LHCP2023)210

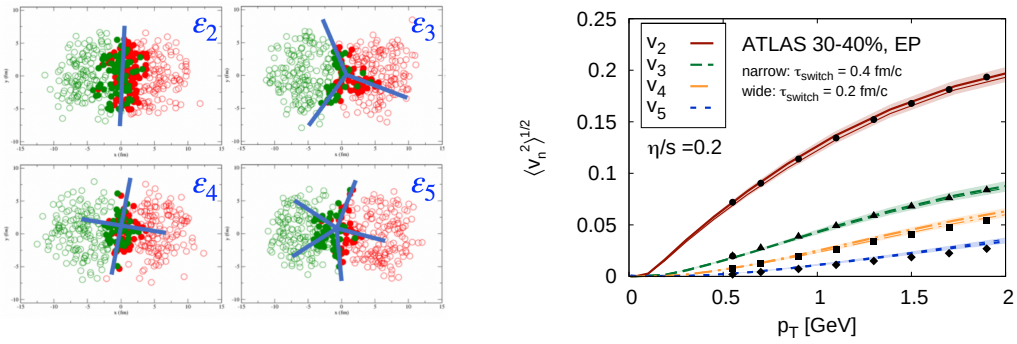

Figure 1: (Color online) Decomposition of the coordinate space anisotropy of the initial overlapping region between two colliding nuclei (left) and different orders of collective flow coefficients of the final state hadrons in the momentum space (right). The figures are taken from Refs. [17, 18].

ε_2. In reality, due to quantum fluctuation of nucleon positions inside a nucleus, this overlapping region can also has triangular, quadrangular, pentagonal and even higher order components whose asymmetries are quantified by ε_3, ε_4, ε_5, etc. These asymmetries generate different pressure gradients of the nuclear matter along different directions in the coordinate space, which are in the end transformed into the momentum space anisotropies of hadrons emitted from the QGP. The collective flow coefficients v_n is defined as the n-th order Fourier coefficients of the particle distribution in the transverse plane:

$$\frac{dN}{d\phi} = \frac{N}{2\pi}\left\{1 + \sum_n 2v_n \cos\left[n\left(\phi - \Phi_n\right)\right]\right\}, \tag{2}$$

with ϕ being the azimuthal angle of the particle momentum and Φ_n denoting the direction of the n-th order event plane (the direction that maximizes v_n). As shown in the right panel of Fig. 1, these collective flow coefficients observed in heavy-ion collisions have been successfully described by relativistic hydrodynamic models [7, 8, 19]. The small specific shear viscosity, or shear-viscosity-to-entropy-density ratio (η/s), extracted from the model-to-data comparison indicates the QGP is a strongly coupled system and displays properties close to an ideal fluid. Recently, the v_2 and v_3 coefficients have also been used to study the non-spherical geometries of different species of nuclei in high-energy collisions [20–22] and even to constrain the size of nucleon inside nucleus [23].

For a systematical and precise extraction of the QGP properties, the Bayesian statistical analysis method has been introduced for model-to-data comparison. For example, in Refs. [24, 25], with Bayesian calibration of hydrodynamic model calculations on the particle yields, flow coefficients, mean p_T's and p_T fluctuations, one can obtain the temperature dependence of both shear and bulk viscosities of the QGP. Note that the ALICE experiment has measured the collective flow coefficients up to the ninth order [26], which will place a more stringent constraint on the QGP properties. The Bayesian calibration on particle yields and collective flows have also been used to extract the equation of state (EoS) of the QGP [27], whose result appears consistent with the lattice QCD prediction.

PoS(LHCP2023)210

The first order collective flow v_1 [28], known as directed flow, is another interesting observable that quantifies the asymmetry between the positive and negative directions along the impact parameter. Phenomenological studies [29, 30] have proposed that non-central nuclear collisions can result in a counterclockwise tilt of the nuclear matter with respect to the beam direction, leading to this asymmetry in the transverse plane at finite rapidity. Detailed model calculations indicate the tilted energy density distribution results in the rapidity-odd v_1 averaged over different hadrons, while the tilted baryon density distribution is crucial for understanding the v_1 splitting between protons and anti-protons [31, 32]. Challenges still remain in understanding v_1 at low beam energies at RHIC [33, 34].

3. Hard probes

Energetic particles can be produced from hard scatterings in both proton-proton (p+p) and nucleus-nucleus (A+A) collisions. Compared to p+p collisions, the spectra of high-energy particles in A+A collisions are modified by the QGP before being observed. This phenomenon is called "jet quenching" and is quantified by the nuclear modification factor $R_{\rm AA}$ as the ratio of particle/jet spectra between A+A and p+p collisions:

$$R_{\rm AA}(y, p_{\rm T}) = \frac{1}{\left\langle N_{\rm coll}^{\rm AA}\right\rangle} \frac{d^2N^{\rm AA}/dydp_{\rm T}}{d^2N^{pp}/dydp_{\rm T}}\,, \tag{3}$$

with $\left\langle N_{\rm coll}^{\rm AA}\right\rangle$ denoting the average number of nucleon-nucleon collisions per A+A collision.

In p+p collisions, the final state hadron spectra can be factorized as [35]

$$d\sigma_h = \sum_{abjd} f_{a/p} \otimes f_{b/p} \otimes d\sigma_{ab\to jd} \otimes D_{h/j}, \tag{4}$$

where $f_{i/p}$ is the parton distribution function (PDF) of parton i inside a proton, $d\sigma_{ab\to jd}$ is the hard partonic cross section for an $ab \to jd$ process, and $D_{h/j}$ is the fragmentation function of forming a hadron h from the parton j. In A+A collisions, without a general proof, the factorization above is extended to

$$d\tilde{\sigma}_h = \sum_{abjj'd} f_{a/A} \otimes f_{b/A} \otimes d\sigma_{ab\to jd} \otimes P_{j\to j'} \otimes \tilde{D}_{h/j'}, \tag{5}$$

where $f_{i/A}$ is known as the nucleus PDF that includes the cold nuclear matter effect (or initial state effect) which can be measured in p+A collisions, $P_{j\to j'}$ represents the medium modification on parton j, and $\tilde{D}_{h/j'}$ is the medium-modified hadronization function. Over the past several decades, tremendous efforts have been devoted in evaluating the parton energy loss ($P_{j\to j'}$) inside the QGP via a combination of elastic and inelastic scatterings. One may refer to Refs. [12, 13, 36, 37] for a detailed comparison between different energy loss formalisms. A multistage jet evolution framework JETSCAPE has been developed [38, 39], which combines different energy loss formalisms according to different regions of phase space they belong to, and performs an end-to-end simulation of jet evolution in relativistic heavy-ion collisions.

By combining parton production and fragmentation at the next-to-leading-order, and elastic and inelastic energy loss of partons inside a hydrodynamic medium, it has been shown within a linear Boltzmann transport (LBT) model that perturbative calculation provides a successful description

PoS(LHCP2023)210

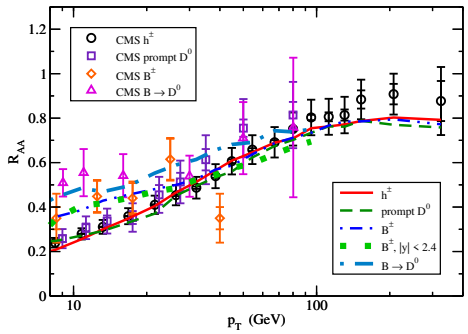

Figure 2: (Color online) Nuclear modification factors of different species of hadrons at high $p_{\rm T}$ in 0-10% Pb+Pb collisions at $\sqrt{s_{\rm NN}}$ = 5.02 TeV. The figure is taken from Ref. [40].

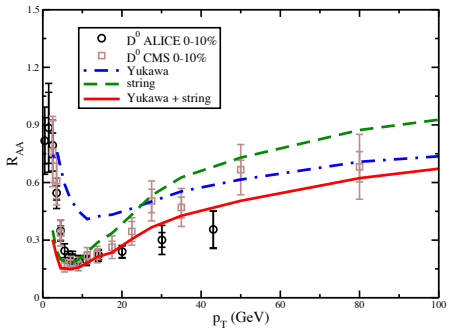

Figure 3: (Color online) Contributions from perturbative and non-perturbative interactions on the D meson $R_{\rm AA}$ in 0-10% Pb+Pb collisions at $\sqrt{s_{\rm NN}}$ = 5.02 TeV. The figure is taken from Ref. [41].

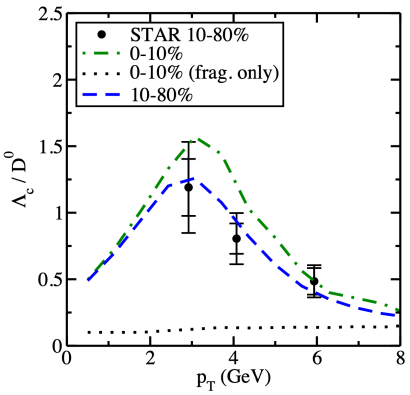

Figure 4: (Color online) The Λ_c/D^0 ratio in Au+Au collisions at $\sqrt{s_{\rm NN}}$ = 200 GeV, compared between different hadronization mechanisms. The figure is taken from Ref. [42].

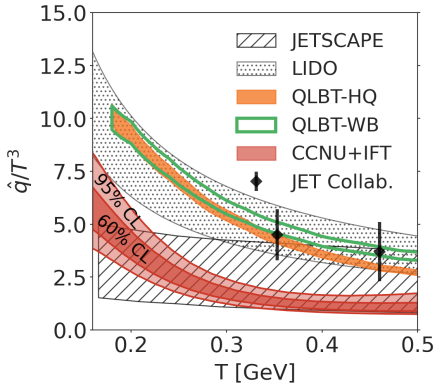

Figure 5: (Color online) The temperature dependence of the jet transport coefficient $\hat{q}$ extracted from different studies. The figure is taken from Ref. [43].

of the $R_{\rm AA}$'s of different species of hadrons at high $p_{\rm T}$ [40]. As shown in Fig. 2, a simultaneous description of $R_{\rm AA}$'s is achieved for charged hadrons, direct D and B mesons, and B-decay D mesons from 8 GeV to very high $p_{\rm T}$. A closer investigation indicates B mesons have a larger $R_{\rm AA}$ than D mesons and charged hadrons below 40 GeV due to the mass effect on parton energy loss. But above 40 GeV, they share similar $R_{\rm AA}$. Future measurements with higher precision will better constrain this momentum dependence of flavor hierarchy of parton energy loss inside the QGP.

As we move to lower $p_{\rm T}$, non-perturbative interactions become important. We have further developed the transport model for heavy quarks by allowing them to scatter with a general potential [41], which contains both a Yukawa term and a string term, representing perturbative and non-perturbative interactions respectively. As shown in Fig. 3, while the Yukawa interaction dominates the heavy meson observables at high $p_{\rm T}$, the string interaction dominates at low $p_{\rm T}$. Their combination provides a good description of heavy flavor phenomenology from low to high $p_{\rm T}$.

At low to medium $p_{\rm T}$, another non-perturbative process is hadronization. In the presence of QGP, there are two major hadronization mechanisms: high $p_{\rm T}$ partons tend to fragment directly

PoS(LHCP2023)210

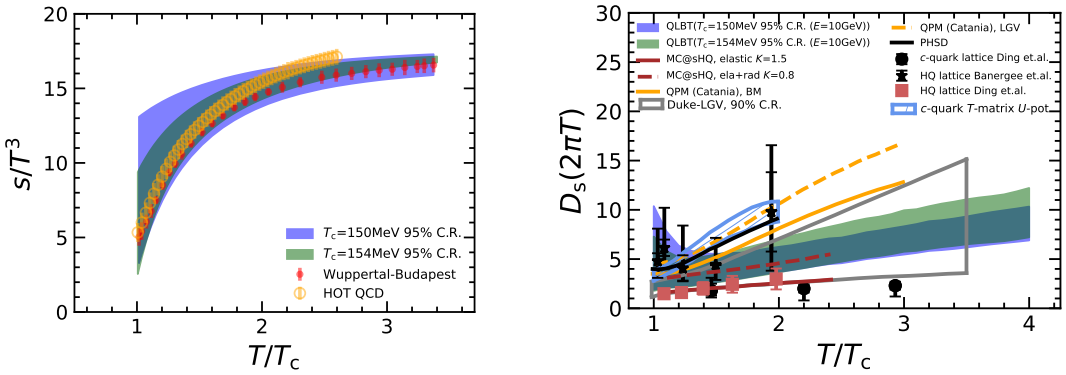

Figure 6: (Color online) The equation of state of the QGP (left) and the spatial diffusion coefficient of heavy quarks (right) extracted from a Bayesian analysis on the heavy meson data in relativistic heavy-ion collisions. The figures are taken from Ref. [54].

into hadrons (fragmentation), while low $p_{\rm T}$ ones prefer combining with thermal partons from the medium to form hadrons (coalescence). As shown in Fig. 4, fragmentation alone cannot describe the baryon-to-meson ratio observed in heavy-ion collisions. Charm quark coalescence with thermal partons from the QGP is essential in understanding these data. One may refer to Ref. [44] for a systematical comparison between different hadronization models. Recently, the CMS experiment has measured $X(3872)$ in heavy-ion collisions [45]. Theoretical studies on hadronization suggest this may provide a novel way of distinguishing between the molecule state and the tetraquark state of exotic particles [46–48]. However, more precise data are required for drawing a conclusion.

Using the sophisticated model calculations above, one can extract various properties of the QGP. The most frequently quoted property related to jets is their transport coefficient $\hat{q}$, defined as the average transverse momentum broadening square of a jet parton per unit length – $d\langle k_\perp^2\rangle/dL$, which is related to the correlation of gluon field between different locations [49]. As shown in Fig. 5, there have been considerable efforts on constraining this $\hat{q}$, ranging from using the traditional least square (χ^2) fitting method (JET) [37], to Bayesian analyses with different ansatzes of the functional form of $\hat{q}$ (JETSCAPE, LIDO, QLBT) [50–52], and then to an information field based Bayesian method that does not rely on a particular functional form of $\hat{q}$ (IFT) [43]. The range of $\hat{q}$ obtained here is an order of magnitude larger than that inside a nucleus extracted from the DIS data [37, 53], indicating the QGP is much more opaque than the cold nuclear matter to jet propagation.

Recently, the EoS of QGP has also been extracted using hard probe observables for the first time [54]. Within the quasi-particle description of the QGP, the coupling strength between quasi-particles determines the heavy quark transport coefficient and further affects their observables. Meanwhile, the coupling strength also determines the effective mass of quasi-particles and affects the EoS of the quasi-particle system. Therefore, one can extract the coupling strength using the heavy flavor data and then use it to calculate the EoS. The left panel of Fig. 6 shows results (blue and green bands) of the EoS we obtain, which agree with the two sets of lattice data. Meanwhile, the right panel shows the spatial diffusion coefficient of heavy quarks constrained from this work, which appears consistent with other model calculations as well as lattice data. Therefore, this provides a proof-of-principle study on a simultaneous constraints on the properties of QGP and hard probes.

PoS(LHCP2023)210

Similarly, the specific shear viscosity of the QGP has been extracted using the high-p_{T} data for the first time in Ref. [55].

The directed flow of heavy mesons also encodes rich physics. While the STAR data [56] show negative slopes of v_1 with respect to rapidity for both D^0 and $\overline{D}^0$ at RHIC, the ALICE data [57] show opposite slopes between D^0 and $\overline{D}^0$ at LHC. Theoretical studies [58, 59] suggest different physics dominates at different beam energies. At RHIC, the tilted geometry of the QGP leads to similar v_1 between D^0 and $\overline{D}^0$. However, at LHC, the geometry becomes almost symmetric, but the electromagnetic field generated by the colliding nuclei becomes much stronger. The latter deflects opposite charges into opposite directions. Therefore, more precise measurement on the D meson v_1 at LHC will provide a better constraint on the evolution profile of the electromagnetic field in these energetic collisions.

Compared to hadron spectra, fully reconstructed jet spectra are more complicated. When a jet parton scatters through the medium, it can emit gluons, and meanwhile knock thermal partons out of the medium and leave energy depletion behind. When daughter partons of these processes approach the thermal energy scale, they become part of the medium and deposit energy into the medium. Since jet partons and the QGP background cannot be cleanly separated in realistic measurements, a fully reconstructed jet contains all these contributions. We call energy deposition and depletion "medium response" or "jet-induced medium excitation", which is naturally included in all jet observables. Medium response has been shown to increase the jet R_{AA} since it introduces medium constituents into jets [60]. It also enhances the jet energy (jet shape) at large radius [61, 62]. Search for unique signatures of medium response becomes a crucial topic. For example, the energy depletion in the direction opposite to jet propagation, known as "diffusion wake", has been proposed as a unique signature [63, 64], which cannot be described by theory calculations without including medium response. In addition, since the QGP medium has richer baryons than a jet in vacuum, medium response can enhance the baryon-to-meson ratio inside a jet in A+A relative to p+p collision [65, 66]. However, these two signals both require very high precision of jet measurements to confirm. More discussions on medium response can be found in Ref. [67].

4. Summary

A brief overview of soft and hard probe theories in relativistic heavy-ion collisions is presented. We see soft hadrons probe the initial geometry and fluctuation, thermal properties, transport coefficients and EoS of the QGP. Heavy quarks and jets probe the perturbative and non-perturbative interactions, hadronization and transport coefficients inside the QGP, and also the EoS of the QGP. More precise data from future LHC and RHIC runs will provide more accurate understanding of nuclear matter under extreme conditions, such as nucleus geometry, parton energy loss, hadron structure, evolution profile of the electromagnetic field and pattern of jet-induced medium excitation.

Acknowledgments

This work was supported by the National Natural Science Foundation of China (NSFC) under Grant Nos. 12175122 and 2021-867.

PoS(LHCP2023)210

References

[1] S. Borsanyi *et al.*, JHEP **1011**, 077 (2010), arXiv:1007.2580.

[2] HotQCD, A. Bazavov *et al.*, Phys. Rev. D **90**, 094503 (2014), arXiv:1407.6387.

[3] M. Gyulassy and L. McLerran, Nucl. Phys. A **750**, 30 (2005), arXiv:nucl-th/0405013.

[4] P. Jacobs and X.-N. Wang, Prog. Part. Nucl. Phys. **54**, 443 (2005), arXiv:hep-ph/0405125.

[5] W. Busza, K. Rajagopal, and W. van der Schee, Ann. Rev. Nucl. Part. Sci. **68**, 339 (2018), arXiv:1802.04801.

[6] H. Elfner and B. Müller, J. Phys. G **50**, 103001 (2023), arXiv:2210.12056.

[7] P. Huovinen, P. F. Kolb, U. W. Heinz, P. V. Ruuskanen, and S. A. Voloshin, Phys. Lett. **B503**, 58 (2001), hep-ph/0101136.

[8] P. F. Kolb and U. W. Heinz, (2003), nucl-th/0305084.

[9] X. Dong, Y.-J. Lee, and R. Rapp, Ann. Rev. Nucl. Part. Sci. **69**, 417 (2019), arXiv:1903.07709.

[10] X. Dong and V. Greco, Prog. Part. Nucl. Phys. **104**, 97 (2019).

[11] X.-N. Wang and M. Gyulassy, Phys. Rev. Lett. **68**, 1480 (1992).

[12] G.-Y. Qin and X.-N. Wang, Int. J. Mod. Phys. **E24**, 1530014 (2015), arXiv:1511.00790.

[13] A. Majumder and M. Van Leeuwen, Prog. Part. Nucl. Phys. **66**, 41 (2011), arXiv:1002.2206.

[14] S. Cao and X.-N. Wang, Rept. Prog. Phys. **84**, 024301 (2021), arXiv:2002.04028.

[15] P. Salabura and J. Stroth, Prog. Part. Nucl. Phys. **120**, 103869 (2021), arXiv:2005.14589.

[16] A. Andronic, P. Braun-Munzinger, K. Redlich, and J. Stachel, Nature **561**, 321 (2018), arXiv:1710.09425.

[17] G.-Y. Qin, Int. J. Mod. Phys. **E24**, 1530001 (2015), arXiv:1502.02554.

[18] C. Gale, S. Jeon, B. Schenke, P. Tribedy, and R. Venugopalan, Phys. Rev. Lett. **110**, 012302 (2013), arXiv:1209.6330.

[19] C. Shen and L. Yan, Nucl. Sci. Tech. **31**, 122 (2020), arXiv:2010.12377.

[20] C. Zhang and J. Jia, Phys. Rev. Lett. **128**, 022301 (2022), arXiv:2109.01631.

[21] J. Jia, Phys. Rev. C **105**, 044905 (2022), arXiv:2109.00604.

[22] B. Bally *et al.*, (2022), arXiv:2209.11042.

[23] G. Giacalone, B. Schenke, and C. Shen, Phys. Rev. Lett. **128**, 042301 (2022), arXiv:2111.02908.

PoS(LHCP2023)210

[24] J. E. Bernhard, J. S. Moreland, and S. A. Bass, Nature Phys. **15**, 1113 (2019).

[25] JETSCAPE, D. Everett *et al.*, Phys. Rev. Lett. **126**, 242301 (2021), arXiv:2010.03928.

[26] ALICE, S. Acharya *et al.*, JHEP **05**, 085 (2020), arXiv:2002.00633.

[27] S. Pratt, E. Sangaline, P. Sorensen, and H. Wang, Phys. Rev. Lett. **114**, 202301 (2015), arXiv:1501.04042.

[28] ALICE, B. Abelev *et al.*, Phys. Rev. Lett. **111**, 232302 (2013), arXiv:1306.4145.

[29] P. Bozek and I. Wyskiel, Phys. Rev. C **81**, 054902 (2010), arXiv:1002.4999.

[30] Z.-F. Jiang, S. Cao, X.-Y. Wu, C. B. Yang, and B.-W. Zhang, Phys. Rev. C **105**, 034901 (2022), arXiv:2112.01916.

[31] P. Bozek, Phys. Rev. C **106**, L061901 (2022), arXiv:2207.04927.

[32] Z.-F. Jiang, X.-Y. Wu, S. Cao, and B.-W. Zhang, Phys. Rev. C **107**, 034904 (2023), arXiv:2301.02960.

[33] STAR, L. Adamczyk *et al.*, Phys. Rev. Lett. **112**, 162301 (2014), arXiv:1401.3043.

[34] STAR, L. Adamczyk *et al.*, Phys. Rev. Lett. **120**, 062301 (2018), arXiv:1708.07132.

[35] J. C. Collins, D. E. Soper, and G. F. Sterman, Nucl. Phys. B **261**, 104 (1985).

[36] S. A. Bass *et al.*, Phys. Rev. **C79**, 024901 (2009), arXiv:0808.0908.

[37] JET, K. M. Burke *et al.*, Phys. Rev. C **90**, 014909 (2014), arXiv:1312.5003.

[38] JETSCAPE, S. Cao *et al.*, Phys. Rev. C **96**, 024909 (2017), arXiv:1705.00050.

[39] J. H. Putschke *et al.*, (2019), arXiv:1903.07706.

[40] W.-J. Xing, S. Cao, G.-Y. Qin, and H. Xing, Phys. Lett. B **805**, 135424 (2020), arXiv:1906.00413.

[41] W.-J. Xing, G.-Y. Qin, and S. Cao, Phys. Lett. B **838**, 137733 (2023), arXiv:2112.15062.

[42] S. Cao *et al.*, Phys. Lett. B **807**, 135561 (2020), arXiv:1911.00456.

[43] M. Xie, W. Ke, H. Zhang, and X.-N. Wang, Phys. Rev. C **108**, L011901 (2023), arXiv:2206.01340.

[44] J. Zhao *et al.*, (2023), arXiv:2311.10621.

[45] CMS, A. M. Sirunyan *et al.*, Phys. Rev. Lett. **128**, 032001 (2022), arXiv:2102.13048.

[46] S. Cho and S. H. Lee, Phys. Rev. C **101**, 024902 (2020), arXiv:1907.12786.

[47] H. Zhang, J. Liao, E. Wang, Q. Wang, and H. Xing, Phys. Rev. Lett. **126**, 012301 (2021), arXiv:2004.00024.

PoS(LHCP2023)210

[48] B. Wu, X. Du, M. Sibila, and R. Rapp, Eur. Phys. J. A **57**, 122 (2021), arXiv:2006.09945, [Erratum: Eur.Phys.J.A 57, 314 (2021)].

[49] A. Kumar, A. Majumder, and J. H. Weber, Phys. Rev. D **106**, 034505 (2022), arXiv:2010.14463.

[50] JETSCAPE, S. Cao *et al.*, Phys. Rev. C **104**, 024905 (2021), arXiv:2102.11337.

[51] W. Ke and X.-N. Wang, JHEP **05**, 041 (2021), arXiv:2010.13680.

[52] F.-L. Liu *et al.*, Eur. Phys. J. C **82**, 350 (2022), arXiv:2107.11713.

[53] P. Ru, Z.-B. Kang, E. Wang, H. Xing, and B.-W. Zhang, Phys. Rev. D **103**, L031901 (2021), arXiv:1907.11808.

[54] F.-L. Liu, X.-Y. Wu, S. Cao, G.-Y. Qin, and X.-N. Wang, Phys. Lett. B **848**, 138355 (2024), arXiv:2304.08787.

[55] B. Karmakar *et al.*, Phys. Rev. C **108**, 044907 (2023), arXiv:2305.11318.

[56] STAR, J. Adam *et al.*, Phys. Rev. Lett. **123**, 162301 (2019), arXiv:1905.02052.

[57] ALICE, S. Acharya *et al.*, Phys. Rev. Lett. **125**, 022301 (2020), arXiv:1910.14406.

[58] Z.-F. Jiang *et al.*, Phys. Rev. C **105**, 054907 (2022), arXiv:2202.13555.

[59] Y. Sun, S. Plumari, and V. Greco, Phys. Lett. B **816**, 136271 (2021), arXiv:2004.09880.

[60] Y. He *et al.*, Phys. Rev. **C99**, 054911 (2019), arXiv:1809.02525.

[61] Y. Tachibana, N.-B. Chang, and G.-Y. Qin, Phys. Rev. **C95**, 044909 (2017), arXiv:1701.07951.

[62] T. Luo, S. Cao, Y. He, and X.-N. Wang, Phys. Lett. **B782**, 707 (2018), arXiv:1803.06785.

[63] W. Chen, S. Cao, T. Luo, L.-G. Pang, and X.-N. Wang, Phys. Lett. B **777**, 86 (2018), arXiv:1704.03648.

[64] Z. Yang, T. Luo, W. Chen, L.-G. Pang, and X.-N. Wang, Phys. Rev. Lett. **130**, 052301 (2023), arXiv:2203.03683.

[65] A. Luo, Y.-X. Mao, G.-Y. Qin, E.-K. Wang, and H.-Z. Zhang, Phys. Lett. B **837**, 137638 (2023), arXiv:2109.14314.

[66] W. Chen, S. Cao, T. Luo, L.-G. Pang, and X.-N. Wang, Nucl. Phys. A **1005**, 121934 (2021).

[67] S. Cao and G.-Y. Qin, Ann. Rev. Nucl. Part. Sci. **73**, 205 (2023), arXiv:2211.16821.

PoS(LHCP2023)210